Betavoltaic Performance of Radiation-Hardened High-Efficiency Si Space Solar Cells

Ruqiang Bao, Peter J. Brand, and Douglas B. Chrisey

***Abstract*—Long-lived and high-energy-density betavoltaics have a great potential as power supplies for remote and hostile environmental conditions, where volume power density and/or power lifetime are very important considerations. In this paper, we provide new results to aid in the design and optimization of betavoltaics made with Si space solar cells and beta sources. The new results were obtained by using a customized low-energy electron accelerator to characterize the radiation-hardened high-efficiency Si space solar cells while varying the electron beam energy and electron beam current density, i.e., electron beam flux. The betavoltaic conversion efficiency of Si space solar cells increases until 60 keV and then decreases with the increasing electron beam energy. The maximum efficiency (6%) obtained at the electron beam energy of 60 keV suggests that Pm-147 would be a good beta source to make high-efficiency nuclear batteries. The radiation ionization energy is ∼3.90 eV per electron–hole pair for Si space solar cells. Some radiation damage-induced performance degradation was also observed when the Si space solar cells were exposed to the bombardment of 62-keV electrons with fluence up to 4.92×10^{18} betas/cm^2, which is equivalent to the radiation from a semi-infinite Pm-147 layer for ∼2.26 years. The results in this paper suggest that beta-particle entrance window, betavoltaic cells' configuration structure, and device properties such as charge carriers' diffusion length are very important factors to be engineered to improve the conversion efficiency for practical betavoltaics.**

***Index Terms*—Betavoltaics, conversion efficiency, low-energy electron accelerator (LEEA), nuclear battery, radiation ionization energy, solar cells.**

I. Introduction

LONG-LIVED and high-energy-density betavoltaics have a great potential as power supplies for remote and even hostile environmental conditions such as in space or remote sensing [1]–[6] or other situations such as implantable cardiac pacemakers [4], [7] where replacing the power supply is very inconvenient. For these applications, volume power density and/or power lifetime are very important considerations. It is also claimed that betavoltaics can be used to trickle-charge conventional batteries and power consumer devices such as cell phones and laptop computers [8]. Since the discovery of the electron voltaic effect [9], betavoltaic devices have been used to harvest the radiation energy from radioisotopes [2], [10]–[12]. Compared to a thermoelectric converter, which operates by converting the radioisotope decay into heat energy and then into electricity, betavoltaic devices convert the energy of nuclear radiation directly into electric power and thus have higher conversion efficiency. Betavoltaics are formed by coupling semiconductor junction devices with high-energy-density and long half-lifetime radioisotopes. Similar to photovoltaics, betavoltaics employ the built-in electric field in the depletion region at the junction in the devices to separate and gather the generated electron-hole pairs (EHPs). However, unlike photovoltaics, betavoltaics do not require an external radiation source. Since betavoltaics convert the kinetic energy of nuclear radiation decays, e.g., beta particles emitted from radioisotopes, into electrical energy, instead of electromagnetic radiation in photovoltaics, the radioisotopes can be packaged together with the betavoltaic devices to form a self-contained source of electric power [13], which can last for years [14], [15]. However, the main concern in betavoltaics is the radiation damage caused by the high-energy beta particles that induce displacement damage, i.e., defects, and result in the concomitant rapid degradation of device performance. For instance, betavoltaics made with silicon and Sr-90 significantly degrade in a single day, which is much shorter than the radioisotope's half-life of 28 years [16], [17], since the energy of beta particles emitted from Sr^{90} is 540 keV, which is much larger than the radiation damage threshold for silicon.

There are tradeoffs in selecting beta sources and junction devices to make betavoltaics. Detailed discussions are available elsewhere [7], [18]. The energy density, the isotope half-lifetime, and the effects of radiation on the junction device need to be simultaneously considered in selecting a beta source and junction combination. Although the beta mass is considerably smaller than that of typical junction materials (∼50 000×), with an estimated displacement energy value of 20 eV, it is still likely that betas can cause displacement damage by primary knock-on collisions. In general, if the maximum energy $E_{\max}$ of beta particles, and subsequent energy transfer, is not significantly higher than the radiation damage threshold E_{th} for displacement, the junction is deemed radiation hard. On the other hand, if the energy is too low, the resultant output power will be too low so that the betavoltaics are useless for many applications. Olsen discussed possible beta sources for betavoltaic energy

Manuscript received October 29, 2011; revised January 8, 2012; accepted January 30, 2012. Date of publication February 28, 2012; date of current version April 25, 2012. This work was supported by the DARPA Micro-Isotope Power Sources Program and Rensselaer Polytechnic Institute start-up funds. The review of this paper was arranged by Editor A. G. Aberle.

R. Bao was with the Department of Materials Science and Engineering, Rensselaer Polytechnic Institute, Troy, NY 12180 USA. He is currently with the IBM Semiconductor Research and Development Center, Hopewell Junction, NY 12533 USA (e-mail: rbao@us.ibm.com).

P. J. Brand is with the Department of Mechanical, Aerospace, and Nuclear Engineering, Rensselaer Polytechnic Institute, Troy, NY 12180 USA (e-mail:brandp@rpi.edu).

D. B. Chrisey is with the Department of Materials Science and Engineering and Departemnt of Biomedical Engineering, Rensselaer Polytechnic Institute, Troy, NY 12180 USA (e-mail: chrisd@rpi.edu).

Color versions of one or more of the figures in this paper are available online at http://ieeexplore.ieee.org.

Digital Object Identifier 10.1109/TED.2012.2187059

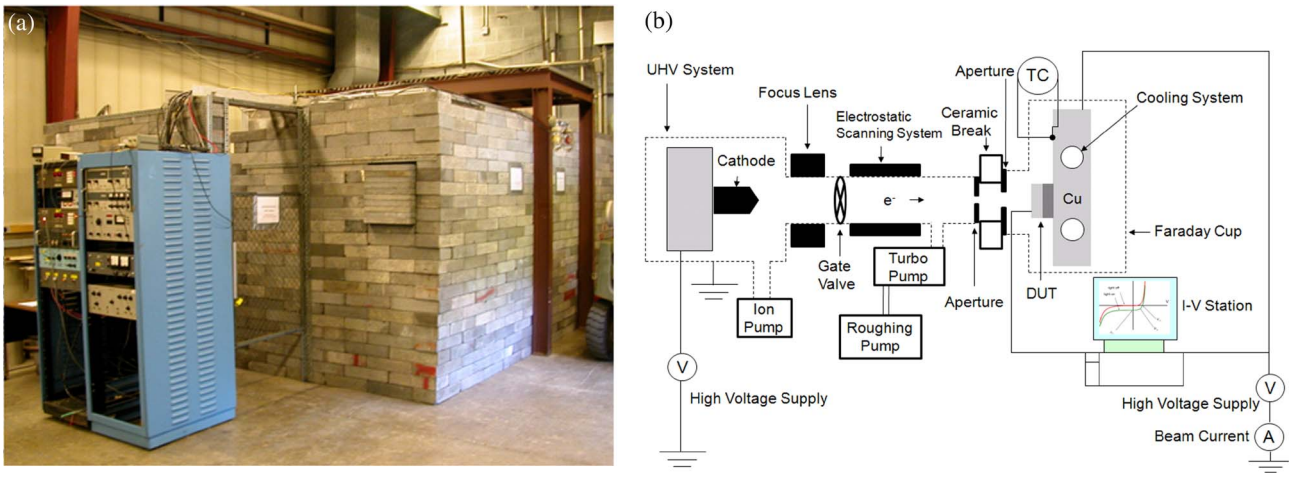

Fig. 1. Customized LEEA at Rensselaer Polytechnic Institute: (a) outlook picture and (b) schematic of LEEA. Here, TC is for thermocouple, DUT is for device under test, and UHV is for ultrahigh vacuum.

conversion [18]. The feasible betavoltaic sources are H-3 [10], [19], Ni-63 [2], and Pm-147 [12] because the $E_{\max}$ in these sources is low enough that radiation effects in many semiconductors can be tolerated. In the case of H-3 and Ni-63, the short-circuit current (and, therefore, output power) is apparently too low for most applications due to the low energy of emitted beta particles and the low specific activity. As a result, betavoltaics powered by H-3 (as once used in pacemakers) have been replaced with long-life batteries [13]. Therefore, among these potential beta sources, Pm-147 appears to be the most promising one for betavoltaic energy conversion. The maximum energy of beta particles emitted from Pm-147 is $\sim$225 keV. Although this value exceeds the approximate threshold ($\sim$145 keV) of Si, the number of electrons having energy above these thresholds is very small [12]. In addition, the half-life of 2.62 years is long enough that a nuclear battery can be fabricated to deliver adequate power for many applications. In the case of junction device selection, three particularly important aspects are the radiation damage threshold, betavoltaic characteristics, and device fabrication. Previous betavoltaic studies involve Si [12], [17], [20]–[23], Ge [17], [23], GaAs [24], SiC [25], [26], diamond [27], GaP [28], GaN [29]–[31], and selenium [23] devices. In theory, the direct band-gap materials such as SiC could be superior to silicon because of their low leakage current, higher radiation damage threshold, and higher conversion efficiency. However, the highly developed Si device technology makes silicon devices a potentially good choice. It is predicted that the betavoltaics made with Si will be much cheaper and more stable than those fabricated by using other materials. Therefore, very recently, more effort is being made to enhance the conversion efficiency of silicon betavoltaics with H-3 [10], [19], Ni-63 [2], and Pm-147 [12], [32] by a 3-D design [32] or a porous structure [20].

Although a lot of work was done on betavoltaics, it is not understood why the conversion efficiency is much lower than the predicted value [10], [16], [32], [33]. The reported maximum conversion efficiency for practical Si-based betavoltaics is only 2.1% [16]. In addition, no robust tools are available to mimic the complicated behavior of beta particles in the devices. Scanning electron microscopy (SEM) was used to characterize the betavoltaic performance of Si junction devices [32] and 4H-SiC devices [34], but the low acceleration voltage ($\leq$30 keV) feature of SEM is not high enough to simulate beta particles emitted from Pm-147 and other radioisotopes. The low current (several microamperes) feature of transmission electron microscopy cannot meet the requirements that the intense electron beam can be utilized to accelerate the lifetime test of devices. In order to be able to mimic high specific activity beta source emitting higher energy beta particles so that the betavoltaic performance and the lifetime of betavoltaic devices can be fully and systematically characterized, a customized low-energy electron accelerator (LEEA), as shown in Fig. 1(a), was designed and built at Rensselaer Polytechnic Institute. In this paper, we used the customized LEEA to investigate the betavoltaic characteristics of high-efficiency Si space solar cells. The performance degradation due to radiation damage by using the accelerated lifetime test mode was also studied. The goal of this paper is to provide new results to aid in the design and optimization of betavoltaics made with Si space solar cells and beta sources.

II. Experimentals

The radiation-hardened high-efficiency Si space solar cells in this paper were received from Naval Research Laboratory and made from a single-crystal silicon substrate and then coated with a dual antireflection layer ($\sim$80-nm thick). The detailed cell structure was described elsewhere [35]–[37]. The 1 sun AM0 performance of Si solar cells was provided by Naval Research Laboratory. Before testing the betavoltaic performance, an additional layer of about 3 nm of graphite was coated by thermal evaporation onto the surface of the Si solar cells in order to minimize backscattering losses from the high-Z metal contact and to remove the discharge of accumulated electrons on the surface of the antireflection layer. The betavoltaic performance of high-efficiency Si space solar cells was characterized *in situ* under irradiation by the LEEA. As schematically shown in Fig. 1(b), the LEEA consists of the ultrahigh vacuum (UHV) system, the thermoelectric electron gun, the high voltage supply, several electromagnetic focusing lens, an electrostatic xy

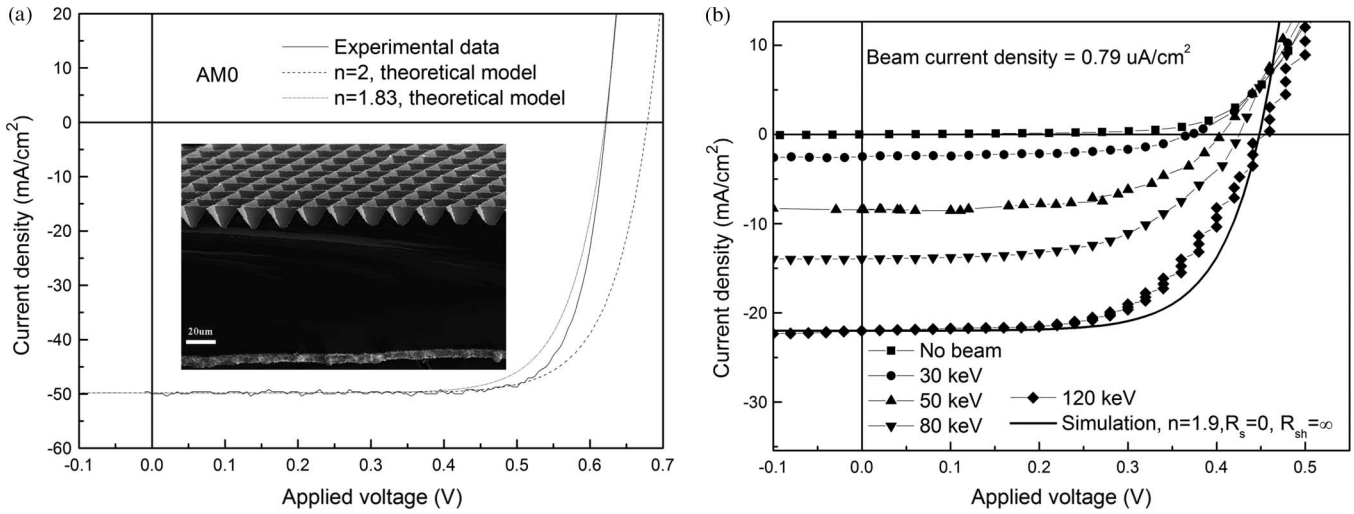

Fig. 2. (a) Photovoltaic and (b) betavoltaic characteristics of high-efficiency Si space solar cells. The inset in (a) is the tilt SEM cross-sectional image of as-received Si space solar cells and shows that the surface of the Si space solar cells was textured with inverted pyramid morphology.

scanning system, apertures, a sample stage, a Faraday cup, and an isolated cooling system. The UHV system is evacuated using an ion pump and a turbo pump. The focusing lenses were used to focus the electrons ejected from the cathode of the electron gun, which was negatively biased by a high voltage supply. The electrostatic scanning system was used to obtain homogenous electron beam irradiation by scanning the beam on the order of 1 kHz vertically and horizontally. The Faraday cup was used to measure the beam current, including the contribution by the backscattered electrons. The isolated cooling system was used to cool down the sample in order to avoid heating due to the bombardment of the high-energy electron beam. The end-station computer was used to control a Keithley 2400 source meter to collect the I–V data. The computer was kept at high voltage and wirelessly controlled. The betavoltaic characteristics as a function of electron beam energy were done with the constant beam current density of 0.79 μA/cm^2. The electron beam current density dependence of betavoltaic response was done with the beam energy of 60 keV. The effect of radiation damage on the betavoltaic performance was conducted by keeping the devices continuously irradiated for about 34.5 h with the electron beam energy of 62 keV and the beam current density of 6.31 μA/cm^2 in the accelerated lifetime test mode. The temperature of the samples during irradiation was 18 °C. Only a 1 °C–2 °C increase in the temperature of the samples for the accelerated lifetime test was observed when the temperature reached the steady state in $\sim$20 min. Hence, the effect of the temperature on the betavoltaic performance is not discussed in this paper. All I–V data were measured *in situ*. The behavior of energetic electrons in materials was modeled by using CASINO, which was detailed in [38].

III. Results and Discussion

The 1 sun AM0 performance of Si solar cells is shown in Fig. 2(a). Short-circuit current density J_{sc} is 49.8 $\pm$ 0.4 mA/cm^2, open-circuit voltage V_{oc} is 0.62 $\pm$ 0.01 V, and power conversion efficiency is 17.9 $\pm$ 0.2%. The inset in Fig. 2(a) is the tilt SEM cross-sectional image of as-received Si solar cells and shows that the top surface of the Si space solar cells was textured with inverted pyramid morphology in order to enhance the conversion efficiency. Under the assumption that the series resistance is zero and the shunt resistance is infinite, the I–V characteristic of Si solar cells is described by

$$J = J_0 \left(\exp\left(\frac{qV}{nkT} \right) - 1 \right) - J_{sc} \tag{1}$$

where J_0 is the reverse saturation current density of the diode, T is the temperature in Kelvin, q is the charge unit, k is Boltzmann's constant, and n is the ideality factor [39]. As shown in Fig. 2(a), the experimental data of Si solar cells deviate from the simulated I–V curves with $n = 2$ in the ideal theoretical model, particularly near the region of V_{oc}, but are close to the simulated I–V curve with $n = 1.83$, which indicates that the space-charge region recombination dominates for the operation. In addition, the assumption is valid because the series and shunt resistances are 0.53 and 1300 Ω/cm^2, respectively, measured from the inverse of slope at V_{oc} and at J_{sc}, respectively.

Betavoltaic responses of Si solar cells as a function of beam energy, when exposed to electron beam irradiation, are shown in Fig. 2(b). The reverse saturation current density J_0 read from the I–V characteristic with no beam is 2.43×10^{-6} A/cm^2. The increase in short-circuit current density with the increasing beam current density and beam energy (equivalent to the increasing input power) indicates that the betavoltaics indeed do a function in a manner analogous to a photovoltaic cell. Similar to photovoltaic characteristics, there is good agreement between the experimental and simulated data when $n = 1.90$, as can be seen from the simulated I–V curve shown in Fig. 2(b), which is relevant to the 120-keV energy. In this case, short-circuit current density was calculated by using the radiation ionization energy of 4.30 eV per EHP. Additional details are described below. The difference between the experimental and simulated data may come from the finite series resistance and shunt resistance, which affect the fill factor (FF). When the electron beam energy is 120 keV with the beam current density

of 0.79 μA/cm^2, the series and shunt resistances are 4 and 325 Ω/cm^2, respectively. The crossover of the I–V curves, as shown in Fig. 2(b), in the forward bias with the increasing beam energy indicates that the higher beam energy reduces the series resistance. This feature is not observed in photovoltaics.

The amount of the generated EHPs depends on the amount of the irradiation particles and the energy of the irradiation particles. In photovoltaics, the absorption of a photon typically generates a single EHP due to the energy of a photon, but in betavoltaics, an incident energetic beta particle can produce hundreds and thousands of EHPs, depending on the energy of the beta particle. For instance, a single beta particle with the energy of 0.7 MeV can produce $\sim 10^5$ EHPs in Si [17]. Generally, the release of the kinetic energy of beta particles into the betavoltaics is completed in two steps. In the first step, the release of kinetic energy creates a nonequilibrium distribution of mobile carriers by inducing transitions from the valence band to the conduction band. This process, called impact ionization, is in competition with phonon generation. In the second step, the excess kinetic energy of the created mobile carriers is transferred to the crystal lattice. The amount of radiation ionization energy consumed per EHP in betavoltaic devices consists of three contributions, i.e., intrinsic bandgap E_g, optical phonon losses, and residual kinetic energy $(\sim 9/5E_g)$ [40]. Therefore, the radiation ionization energy ε is band-gap dependent and can be expressed as

$$\varepsilon \approx E_g + \frac{9}{5}E_g + r(\omega R) \tag{2}$$

where $r(\omega R)$ represents the optical phonon losses and is in the range of 0.5–1 eV [40]. For silicon, ε is 3.6 eV, which was incidentally determined by using alpha particles to bombard pure silicon [41], [42]. Therefore, the maximum possible current density $J_{\max}$ that can be collected under short-circuit condition is given by

$$J_{\max} = q\phi_0 \frac{E}{\varepsilon} \tag{3}$$

where ϕ_0 is the incident beta-particle flux and E is the beta-particle energy [18]. However, the incident beta particles in betavoltaics are partially reflected from or near the semiconductor surface and do not contribute to the generation of EHPs and to the output current. Meanwhile, only the EHPs generated within the depletion region and in the range of the carrier's diffusion length near the depletion region can be collected to produce the output current in betavoltaic devices [14]. Therefore, the $J_{\rm sc}$ for betavoltaics can be given by

$$J_{\rm sc} = (1-r)QJ_{\max} \tag{4}$$

where r is the reflection coefficient for beta particles from the semiconductor surface and Q is the collection efficiency of the devices [18]. The beta-particle reflection primarily depends on the atomic number of the material. For Si, $r = 0.1$ [43]. Q is a function of the beta-particle properties, the semiconductor properties, and the device properties. Q can approach 0.8–1 for silicon when the beta source is Pm-147 [18].

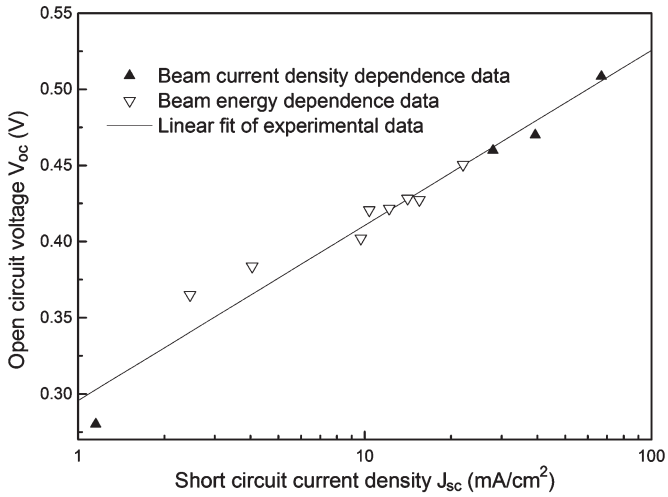

Fig. 3. Relationship of open-circuit voltage $V_{\rm oc}$ versus short-circuit current density $J_{\rm sc}$ for beam current density dependence and beam energy dependence.

The $V_{\rm oc}$ in betavoltaic response can be connected to $J_{\rm sc}$ by the well-known relation [44]

$$V_{\rm oc} = \frac{nkT}{q}\ln\left(\frac{J_{\rm sc}}{J_0}\right) \text{ for } J_{\rm sc} \gg J_0. \tag{5}$$

As shown in Fig. 3, the relationship between $V_{\rm oc}$ and $J_{\rm sc}$ follows (5). The ideal factor $(n = 1.9)$ is extracted from the slope of linear fitting of experimental data. The condition of $r = 0.1$ and $n = 1.9$ is used in later section for the comparison between experimental and calculated data.

The FF [45] and overall efficiency η [18] can be given, respectively, by

$$\text{FF} = \text{FFs}\left(1 - \frac{\frac{V_{\rm oc}}{nkT/q} + 0.7}{\frac{V_{\rm oc}}{nkT/q}}\frac{\text{FFs}}{\frac{R_{\rm sh}}{V_{\rm oc}/J_{\rm sc}}}\right) \tag{6}$$

$$\eta = 100(1-r)Q\left(\frac{V_{\rm oc}\text{FF}}{\varepsilon}\right)\% \tag{7}$$

where

$$\text{FFs} = \left(\frac{\left(\frac{V_{\rm oc}}{nkT/q} - \ln\left(\frac{V_{\rm oc}}{nkT/q} + 0.72\right)\right)}{\frac{V_{\rm oc}}{nkT/q} + 1}\right) \times \left(1 - \frac{1.1R_s}{V_{\rm oc}/J_{\rm sc}}\right) + \frac{\left(\frac{1.1R_s}{V_{\rm oc}/J_{\rm sc}}\right)^2}{5.4}$$

where R_s is the series resistance and $R_{\rm sh}$ is the shunt resistance. The experimental and calculated $V_{\rm oc}$, $J_{\rm sc}$, and η by using the above equations are shown in Fig. 4. Here, the series resistance $(4\ \Omega/\text{cm}^2)$, the shunt resistance $(325\ \Omega/\text{cm}^2)$, and the reflection coefficient $(r = 0.1)$ were used for the calculations. The condition of collection efficiency and radiation ionization energy for the calculations is displayed in Fig. 4. It is shown in Fig. 4(a) that higher beam energy has higher short-circuit current density. Similarly, although not shown here, a higher beam current density leads to a higher short-circuit current density as well. Two boundary limits are also plotted in Fig. 4(a). If all generated EHPs are collected by the devices, i.e., $Q = 1$, and

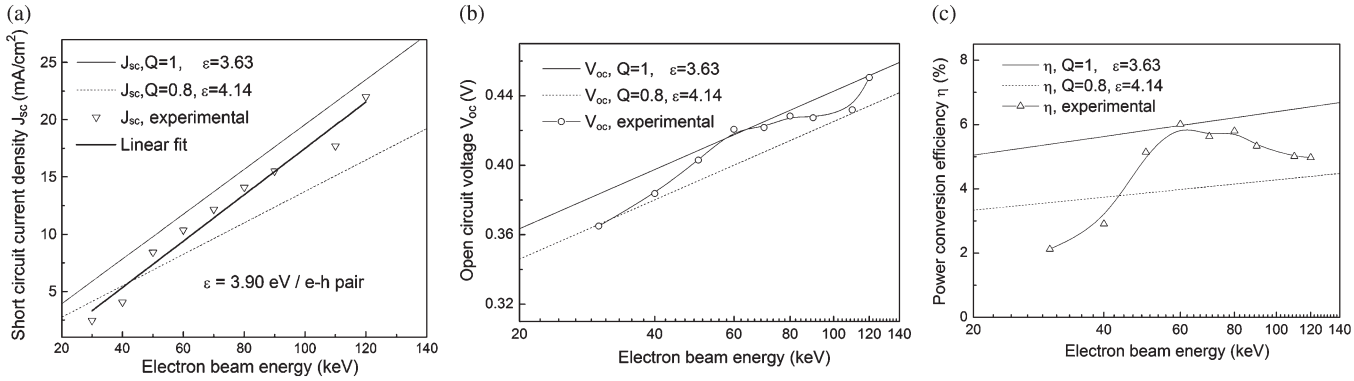

Fig. 4. Experimental and calculated betavoltaic performance as a function of electron beam energy (a) $J_{\rm sc}$ versus E, (b) $V_{\rm oc}$ versus E, and (c) η versus E. The boundary limits are calculated by using $r = 0.1$ and $n = 1.90$. Here, the electron beam current density is 0.79 μA/cm^2 for experimental data.

TABLE I
EFFECTIVE IONIZATION ENERGY ε AT DIFFERENT BEAM ENERGY VALUES WITH BEAM CURRENT DENSITY OF 0.79 μA/cm^2

E (keV)	30	40	50	60	70	80	90	110	120
$\mathcal{E}$ (eV)	9.65	7.80	4.69	4.57	4.54	4.48	4.58	4.91	4.31

if one EHP consumes the minimum energy, i.e., $\varepsilon = 3.63$ eV, the possible maximum $J_{\rm sc}$ (solid line) is obtained. On the other hand, the condition of $Q = 0.8$ and $\varepsilon = 4.14$ eV gives the possible minimum $J_{\rm sc}$ (dot line). As shown in Fig. 4(a), $J_{\rm sc}$ falls in the predicted region when the beam energy is larger than 40 keV. When the beam energy is lower than 40 keV, $J_{\rm sc}$ is lower than the possible minimum $J_{\rm sc}$. The reason could be that the antireflection layer and the electrical collection electrode consume certain energy of electron beam when the energetic electrons penetrate through these layers to reach effective junction device. In order to compensate the energy consumed by the antireflection layer and the electrical collection electrode and to remove the effect of Q and r on the output short-circuit current density, radiation ionization energy ε is extracted from the reciprocal slope of the linear fit of experimental data. The extracted ε is $\sim$3.90 eV, which falls in the range of 3.63–4.14 eV, although it is a little higher than 3.60 eV. This result indicates that the betavoltaic response of Si solar cells matches the theoretical prediction. Effective radiation ionization energy ε is calculated directly by dividing the product of incident beam current density and the corresponding energy by the short-circuit current density. The effective radiation ionization energy under different beam energy conditions is listed in Table I. It is shown in Table I that, for low-energy beam case (<40 keV), the effective radiation ionization energy is much higher than the theoretical value, as expressed in (2). For higher energy beam case, the apparent radiation ionization energy is still higher than the theoretical values, but it is close to the maximum theoretical value of 4.14 eV. The positive intercept of the linear fit of experimental data at the electron beam energy axis also indicates that the antireflection layer and the electrical collection electrode consume certain energy of electron beams.

As shown in Fig. 4(b), $V_{\rm oc}$ increases with the increasing electron beam energy. Because $J_{\rm max}$ has a linear relationship with the electron beam energy, $V_{\rm oc}$ has a logarithmic relationship of electron beam energy if r and Q are not changed. It is shown in Fig. 4(c) that conversion efficiency η increases with the electron beam energy up to 60 keV and then decreases with the electron beam energy. As shown in Fig. 4(b), although there is certain fluctuation, except for the energy at 60 keV, $V_{\rm oc}$ falls in the range calculated by using $Q = 1$, $\varepsilon = 3.63$ eV and $Q = 0.8$, $\varepsilon = 4.14$ eV. The η and $V_{\rm oc}$ values obtained at 60-keV electron beam energy are hitting or a little bit higher than the upper boundary. The reasons are not clear and could be related to the parameters, such as reverse saturation current density and the ideal factor, used for the analytical calculations, and the measurement and control tools of LEEA. Further analysis is needed to find the root cause. For energy values lower than 40 keV, the conversion efficiency is lower than the expected efficiency. The conversion efficiency at 30 keV is $\sim$2.12% but still higher than the reported value (1.02%) for 3-D silicon betavoltaics characterized via SEM at the acceleration voltage of 30 kV [32]. When the electron beam energy is 60 keV, the maximum experimental η is obtained and is 6.01%, which is higher than that reported for Pm_2O_3/Si n^+p betavoltaics in which the maximum conversion efficiency is only 2.1% [16]. For practical betavoltaics, the beta source efficiency should be included, which expresses the fraction of all betas created that are actually emitted from the source and directed toward the device [18]. The average energy of beta particles emitted from Pm-147 is $\sim$62 keV. The present results suggest that Pm-147 would be a good beta source to make a high-efficiency nuclear battery with Si solar cells.

In betavoltaic devices, junction depth plays a critical role to determine the short-circuit current density and the conversion efficiency. Junction depth determines the location to collect the generated EHPs in the device and thus has a great impact on the conversion efficiency since the penetration depth of the energetic beta particles is energy dependent. In order to understand the behavior of energetic electrons in Si space solar cells, the trajectory of electrons in a planar material stack model was studied by using CASINO. Here, the electrons hit the sample vertically. The schematic of the sample model is shown in the right-lower inset in Fig. 5(a), and the materials and the corresponding thickness and density are shown therein as well. As shown in Fig. 5(a), the electron range increases with the beam energy. The ranges for 60- and 120-keV electrons are 15.9 and 53.9 μm, respectively. The distribution of electrons that stopped in the sample along the depth follows a Gaussian

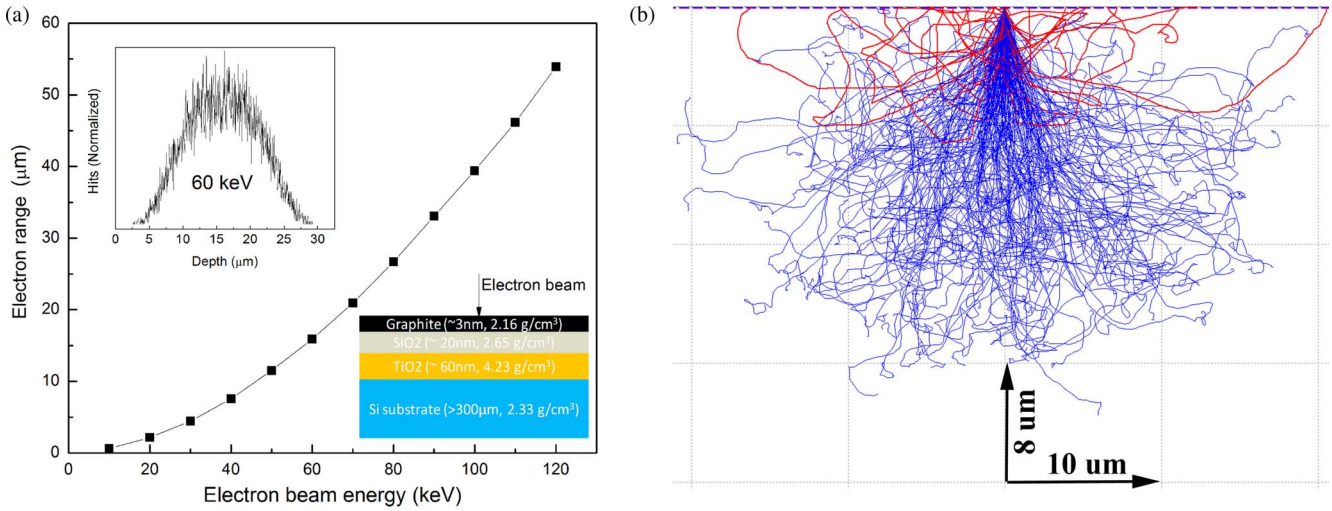

Fig. 5. Behavior of energetic electrons in the proposed material stack simulated by using CASINO code: (a) range of energetic electrons as a function of energy and (b) trajectory of electrons with the energy of 60 keV. The left-upper inset in (a) shows the distribution of electrons with the energy of 60 keV in the proposed material stack, which is shown with the corresponding thickness and density in the right-lower inset in (a). The red lines in (b) represent the trajectory of backscattered electrons.

distribution, as shown in the left-upper inset in Fig. 5(a). The maximum penetration depth in the sample is about double the electron range. As an example, the trajectory (purple line) of electrons in the sample with the energy of 60 keV is shown in Fig. 5(b), in which the red line shows the trajectory of the backscattered electrons in the sample. For lightly doped Si ($\sim 1 \times 10^{16}$ cm^3), the diffusion length L_p of holes in n-type Si and the diffusion length L_n of electrons in p-type Si are 30 μm [46] and 50 μm [47], respectively. For Si solar cells, n^+/p or p^+/n junction devices are generally used to enhance the conversion efficiency [48]. The former physical structure is preferred because of the higher minority (electron) lifetime and diffusion length, which are more important for betavoltaic devices, in the p-type substrate where most of EHPs are generated. The top diffused layer of high doping concentration is about 1 μm or less [14]. In the case of low-energy electrons, the generated EHPs, which can contribute to the output current, are reduced because some energy is consumed by the antireflection layer and the electrode. As a result, the conversion efficiency is reduced. With the increase of electron beam energy, the portion of the generated EHPs that can contribute to the output current increases so that the conversion efficiency increases. However, if the energy of electron beam further increases, the conversion efficiency decreases because part of the generated EHPs cannot be collected at the junction because of the large electron range. Take 120-keV electrons as an example. The maximum penetration depth is about 100 μm; however, the larger minority diffusion length is only about 53.9 μm. Therefore, the EHPs generated at the depth of 100 μm are unable to make contribution to the output current if the depletion region cannot reach 47 μm deep. In the current case, the junction depth is $\sim$0.15 μm [35], [37] and the depletion width does not exceed 1 μm. Therefore, the EHPs generated at the depth larger than $\sim$55 μm do not contribute to the output current and the conversion efficiency is reduced. However, these EHPs increase the conductivity of semiconductor substrate and thus reduce the series resistance, as indicated by the crossover of the I–V curves in Fig. 2(a). Therefore, diffusion length is a critical parameter for betavoltaics to improve the conversion efficiency. Increasing effective depletion width and diffusion length can help improve the conversion efficiency. Based on this point, 3-D junction devices [32], porous junction devices [10], or multijunction device stack are desirable to enhance the conversion efficiency by collecting the generated EHPs more effectively. Meanwhile, the sandwich stack of device/beta source/device can enhance the conversion efficiency as well.

In order to investigate the effect of radiation damage on the betavoltaic performance, the Si solar cell was continuously bombarded by 62-keV electron beam with beam current density of 6.31 μA/cm^2 until the fluence reached 4.92×10^{18} betas/cm^2, which is equivalent to the radiation from a semi-infinite Pm-147 layer for $\sim$2.26 years. Betavoltaic I–V characteristics at different fluences are shown in Fig. 6(a). It can be seen that some performance degradation induced by radiation damage with the increasing fluence can be observed because I–V characteristics shift, gradually but very slowly, toward the origin with the increasing fluence. As shown in Fig. 6(b), maximum output power $P_{\max}$ (which determines the power conversion efficiency), short-circuit current density $J_{\rm sc}$, and open circuit voltage $V_{\rm oc}$ degrade a little with the increasing radiation fluence. The degradation coefficients for them are 9.32×10^{-22} mW $\cdot$ cm^2/betas, 4.65×10^{-22} mA/betas, and 7.53×10^{-22} V $\cdot$ cm^2/betas, respectively. The higher degradation coefficient for the maximum output power is probably caused by the reduction of FF.

The performance degradation is a result of radiation-induced defects, via primary knock-on collision, which give rise to the energy states in the band gap. It is these defect states that have a major impact on the electrical behavior of semiconductor materials and devices by affecting several processes, including recombination and scattering. Radiation-induced recombination centers decrease the lifetime of charge carriers, and radiation-induced scattering centers cause the mobility to decrease. Hence, these two kinds of defects decrease charge

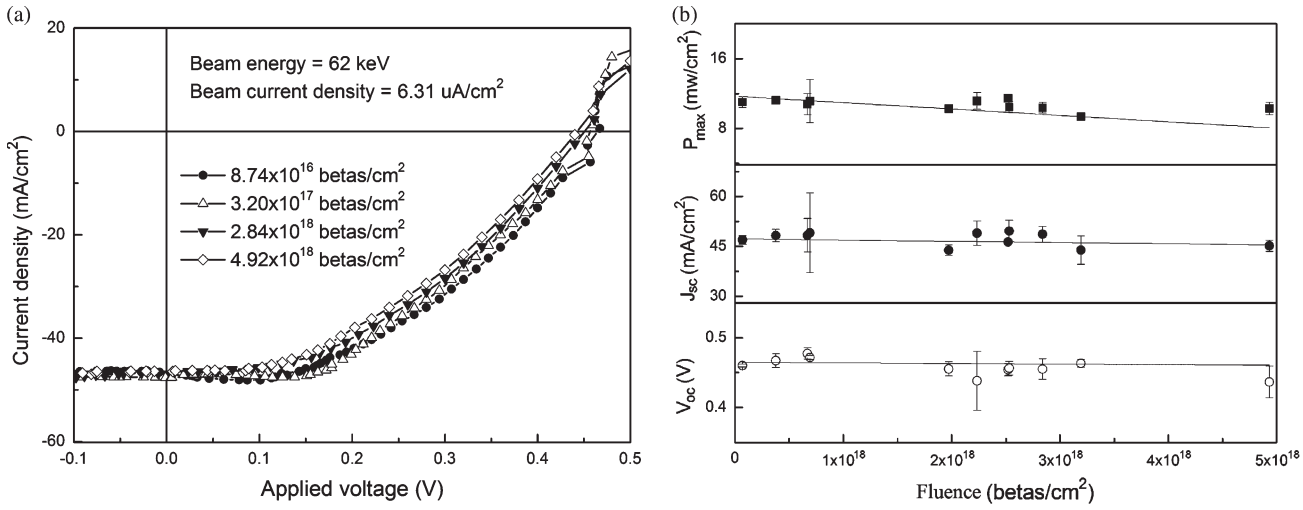

Fig. 6. Effect of radiation damage on the betavoltaic performance of Si space solar cells under the bombardment of electrons with the beam energy of 62 keV and the beam current density of 6.31 μA/cm^2. (a) I–V characteristics at different fluence levels. (b) Maximum output power $P_{\max}$, short-circuit current density $J_{\rm sc}$, and open-circuit voltage $V_{\rm oc}$ as a function of the fluence.

carriers' diffusion length and thus degrade the betavoltaic performance. In addition, depending on the energy and flux of beta particles, relatively widely spaced defects or a number of more closely spaced defects may be produced. Following their creation, defects will reorder to more stable positions by annealing processes. Similar to increasing temperature, increasing injection level will enhance such defect annealing processes [49]. Hence, the effect of higher energy electron beam and electron beam flux levels on the degradation of high-efficiency Si solar cells needs to be studied in the future to provide the information to optimize the design of betavoltaics. Further investigation is needed to correlate the displacement damage with the nonionizing energy loss in order to be able to predict the radiation-induced degradation.

IV. Conclusion

In this paper, we have provided new results to aid in the design and optimization of betavoltaics made with Si space solar cells and beta sources. These results were obtained by using a customized LEEA to characterize the betavoltaic performance of radiation-hardened high-efficiency Si space solar cells. The effective radiation ionization energy of Si space solar cells is $\sim$3.90 eV per EHP. The betavoltaic conversion efficiency increases and then decreases with the increasing electron beam energy. The maximum efficiency (6.01%) obtained at the electron beam energy of 60 keV suggests that Pm-147 would be a good beta source to make a high-efficiency nuclear battery. Some radiation damage-induced performance degradation was also observed when the Si space solar cells were exposed to the bombardment of 62-keV electrons with the fluence up to 4.92×10^{18} betas/cm^2, which is equivalent to the radiation from a semi-infinite Pm-147 layer for $\sim$2.26 years. In this paper, the capability of LEEA to characterize the betavoltaic performance and the accelerated lifetime test of betavoltaic devices was clearly demonstrated as well.

In order to improve the conversion efficiency of betavoltaics, four key factors should be considered. The optimization of the particle entrance window and the window materials is important, particularly for low-energy electrons, since the antireflection layer and the electrical collection electrode consume part of the electron energy. Otherwise, nonnegligible energy is lost from the beginning and the conversion efficiency is low. A device configuration structure should be optimized to enhance the conversion efficiency, particularly for the higher energy electrons, because of their long penetration depth in the devices. Three-dimensional junction devices, porous junction devices, and/or multijunction device stacks are desirable. Furthermore, devices should be engineered to improve the diffusion length in order to have Q close to 1. In addition, betavoltaic cells should be designed to reduce the self-absorption of emitted betas, which is a very important consideration for practical betavoltaics.

Acknowledgment

The authors would like to thank Dr. S. Messenger of Naval Research Laboratory for providing the high-efficiency Si space solar cells; Prof. A. N. Caruso of the University of Missouri at Kansas City for the very helpful discussion of the characterization and calculation; A. Haberl of the University at Albany Ion Beam Laboratory and the Support Staff of RPI Gaerttner LINAC Laboratory; and M. C. Gray, M. R. Strock, and A. Kerdoun for their great work in setting-up LEEA and their help during the characterization of betavoltaic performance.

References

[1] W. R. Corliss and D. G. Harvey, *Radioisotopic Power Generation*. Englewood Cliffs, NJ: Prentice-Hall, 1964.
[2] B. Ulmen, P. D. Desai, S. Moghaddam, G. H. Miley, and R. I. Masel, "Development of diode junction nuclear battery using 63Ni," *J. Radioanal. Nucl. Chem.*, vol. 282, no. 2, pp. 601–604, Nov. 2009.
[3] C. Knight, J. Davidson, and S. Behrens, "Energy options for wireless sensor nodes," *Sensors*, vol. 8, no. 12, pp. 8037–8066, Dec. 2008.
[4] R. Duggirala, H. Li, and A. Lal, "High efficiency beta radioisotope energy conversion using reciprocating electromechanical converters with integrated betavoltaics," *Appl. Phys. Lett.*, vol. 92, no. 15, pp. 154104-1–154104-3, Apr. 2008.

[5] C. D. Cress, B. J. Landi, R. P. Raffaelle, and D. M. Wilt, "InGaP alpha voltaic batteries: Synthesis, modeling, and radiation tolerance," *J. Appl. Phys.*, vol. 100, no. 11, pp. 114519-1–114519-5, Dec. 2006.
[6] P. M. Brown, "Solid state radioisotopic energy converter for space nuclear power," in *AIP Conf. Proc.*, 1993, vol. 271, pp. 325–331.
[7] L. C. Olsen, "Betavoltaic energy conversion," *Energy Convers.*, vol. 13, no. 4, pp. 117–124, Dec. 1973.
[8] . [Online]. Available: http://www.betavoltaic.co.uk/laptop_battery.html
[9] W. Ehrenberg, C. S. Lang, and R. West, "The electron voltaic effect," *Proc. Phys. Soc. A*, vol. 64, no. 4, p. 424, Apr. 1951.
[10] W. Sun, N. P. Kherani, K. D. Hirschman, L. L. Gadeken, and P. M. Fauchet, "A three-dimensional porous silicon p-n diode for betavoltaics and photovoltaics," *Adv. Mater.*, vol. 17, no. 10, pp. 1230–1233, May 2005.
[11] A. Kavetskiy, G. Yakubova, S. M. Yousaf, K. Bower, J. D. Robertson, and A. Garnov, "Efficiency of Pm-147 direct charge radioisotope battery," *Appl. Radiat. Isot.*, vol. 69, no. 5, pp. 744–748, May 2011.
[12] H. Flicker, J. J. Loferski, and T. S. Elleman, "Construction of a promethium-147 atomic battery," *IEEE Trans. Electron Devices*, vol. ED-11, no. 1, pp. 2–8, Jan. 1964.
[13] D. Emin, "Unusual properties of icosahedral boron-rich solids," *J. Solid State Chem.*, vol. 179, no. 9, pp. 2791–2798, Sep. 2006.
[14] L. S. Wei, "Parametric studies and optimization of the beta-voltaic cell–I. Short-circuit current," *Solid State Electron.*, vol. 17, no. 10, pp. 1091–1098, Oct. 1974.
[15] L. S. Wei, "Parametric studies and optimization of the beta-voltaic cell–II open-circuit voltage and power efficiencies," *Solid State Electron.*, vol. 18, no. 1, pp. 71–77, Jan. 1975.
[16] W. G. Pfann and W. V. Roosbroeck, "Radioactive and photoelectric p-n junction power sources," *J. Appl. Phys.*, vol. 25, no. 11, pp. 1422–1434, Nov. 1954.
[17] P. Rappaport, "The electron-voltaic effect in p-n junctions induced by beta-particle bombardment," *Phys. Rev.*, vol. 93, no. 1, pp. 246–247, Jan. 1954.
[18] L. C. Olsen, "Review of betavoltaic energy conversion," in *Proc. 12th Space Photovolt. Res. Technol. Conf.*, 1993, pp. 256–267.
[19] T. Kosteski, N. P. Kherani, P. Stradins, F. Gaspari, W. T. Shmayda, L. S. Sidhu, and S. Zukotynski, "Tritiated amorphous silicon betavoltaic devices," *Proc. Inst. Elect. Eng.—Circuits Devices Syst.*, vol. 150, no. 4, pp. 274–281, Aug. 2003.
[20] J. P. Clarkson, W. Sun, K. D. Hirschman, L. L. Gadeken, and P. M. Fauchet, "Betavoltaic and photovoltaic energy conversion in three-dimensional macroporous silicon diodes," *Phys. Stat. Sol. (A)*, vol. 204, no. 5, pp. 1536–1540, May 2007.
[21] L. C. Olsen, "Beta irradiation of silicon junction devices: Effects on diffusion length," *IEEE Trans. Nucl. Sci.*, vol. NS-19, no. 6, pp. 375–381, Dec. 1972.
[22] R. C. Woodbury, R. A. Van Epps, and D. I. Olson, "Radiation hardening of electron voltaic cells," *IEEE Trans. Nucl. Sci.*, vol. NS-25, no. 6, pp. 1479–1482, Dec. 1978.
[23] P. Rappaport, J. J. Loferski, and E. G. Linder, "The electron voltaic effect in germanium and silicon p-n junctions," *RCA Rev.*, vol. 17, pp. 100–128, Mar. 1956.
[24] H. Chen, L. Jiang, and X. Chen, "Design optimization of GaAs betavoltaic batteries," *J. Phys. D, Appl. Phys.*, vol. 44, no. 21, p. 215303, Jun. 2011.
[25] Q. Da-Yong, Y. Wei-Zheng, G. Peng, Y. Xian-Wang, Z. Bo, Z. Lin, G. Hui, and Z. Hong-Jian, "Demonstration of a 4H-SiC betavoltaic nuclear battery based on Schottky barrier diode," *Chinese Phys. Lett.*, vol. 25, no. 10, pp. 3798–3800, Oct. 2008.
[26] C. J. Eiting, V. Krishnamoorthy, S. Rodgers, T. George, J. D. Robertson, and J. Brockman, "Demonstration of a radiation resistant, high efficiency SiC betavoltaic," *Appl. Phys. Lett.*, vol. 88, no. 6, pp. 064101-1–064101-3, Feb. 2006.
[27] D. M. Trucchi, E. Cappelli, and P. Ascarelli, "Designing CVD diamond betavoltaic batteries," in *Proc. 13th Italian Conf. Sens. Microsyst.*, Roma, Italy, 2008, pp. 459–463.
[28] P. E. Sims, L. C. Dinetta, and A. M. Barnett, "High efficiency GaP power conversion for betavoltaic applications," in *Proc. 13th Space Photovolt. Res. Technol. Conf.*, 1994, pp. 373–382.
[29] M. Lu, G. Zhang, K. Fu, G. Yu, D. Su, and J. Hu, "Gallium nitride Schottky betavoltaic nuclear batteries," *Energ. Convers. Manag.*, vol. 52, no. 4, pp. 1955–1958, Apr. 2011.
[30] Z. Cheng, H. San, Y. Li, and X. Chen, "The design optimization for GaN-based betavoltaic microbattery," in *Proc. 5th IEEE Int. Conf. Nano/Micro Eng. Mol. Syst.*, 2010, pp. 582–586.
[31] C. Honsberg, W. A. Doolittle, M. Allen, and C. Wang, "GaN betavoltaic energy converters," in *Conf. Rec. 31st IEEE Photovolt. Spec. Conf.*, 2005, pp. 102–105.
[32] R. Duggirala, S. Tin, and A. Lai, "3D silicon betavoltaics microfabricated using a self-aligned process for 5 milliwatt/CC average, 5 year lifetime microbatteries," in *Proc. Int. Solid-State Sens., Actuators Microsyst. Conf.*, 2007, pp. 279–282.
[33] M. V. S. Chandrashekhar, C. I. Thomas, H. Li, M. G. Spencer, and A. Lal, "Demonstration of a 4H SiC betavoltaic cell," *Appl. Phys. Lett.*, vol. 88, no. 3, pp. 033506-1–033506-3, Jan. 2006.
[34] M. V. S. Chandrashekhar, C. I. Thomas, and M. G. Spencer, "Measurement of the mean electron–hole pair ionization energy in 4H SiC," *Appl. Phys. Lett.*, vol. 89, no. 4, pp. 042113-1–042113-3, Jul. 2006.
[35] H. Washio, T. Katsu, Y. Tonomura, T. Hisamatsu, T. Saga, T. Matsutani, A. Suzuki, Y. Yamamoto, and S. Matsuda, "Development of high efficiency thin silicon space solar cells," in *Conf. Rec. IEEE Photovolt. Spec. Conf.*, 1993, pp. 1347–1351.
[36] T. Katsu, K. Shimada, H. Washio, Y. Tonomura, T. Hisamatsu, K. Kamimura, T. Saga, T. Matsutani, A. Suzuki, O. Kawasaki, Y. Yamamoto, and S. Matsuda, "Development of high efficiency silicon space solar cells," in *Conf. Rec. IEEE Photovolt. Spec. Conf.*, 1994, pp. 2133–2136.
[37] A. Suzuki, "High-efficiency silicon space solar cells," *Solar Energy Mater. Solar Cells*, vol. 50, no. 1–4, pp. 289–303, Jan. 1998.
[38] D. Drouin, A. Couture, D. Joly, X. Tastet, V. Aimez, and R. Gauvin, "CASINO V2.42—A fast and easy-to-use modeling tool for scanning electron microscopy and microanalysis users," *Scanning*, vol. 29, no. 3, pp. 92–101, May 2007.
[39] D. K. Schroder, *Semiconductor Material and Device Characterization.*, 3rd ed. Hoboken, NJ: Wiley, 2006.
[40] C. A. Klein, "Bandgap dependence and related features of radiation ionization energies in semiconductors," *J. Appl. Phys.*, vol. 39, no. 4, pp. 2029–2038, Mar. 1968.
[41] K. G. McKay and K. B. McAfee, "Electron multiplication in silicon and germanium," *Phys. Rev.*, vol. 91, no. 5, pp. 1079–1084, Sep. 1953.
[42] P. A. Wolff, "Theory of electron multiplication in silicon and germanium," *Phys. Rev.*, vol. 95, no. 6, pp. 1415–1420, Sep. 1954.
[43] P. Rappaport and E. G. Linder, "Radioactive charging effects with a dielectric medium," *J. Appl. Phys.*, vol. 24, no. 9, pp. 1110–1114, Sep. 1953.
[44] M. Shur, *Physics of Semiconductor Devices*. Englewood Cliffs, NJ: Prentice-Hall, 1990.
[45] M. A. Green, "Accuracy of analytical expressions for solar cell fill factors," *Solar Cells*, vol. 7, no. 3, pp. 337–340, Dec. 1982.
[46] M. S. Tyagi and R. V. Overstraeten, "Minority carrier recombination in heavily-doped silicon," *Solid State Electron.*, vol. 26, no. 6, pp. 577–597, Jun. 1983.
[47] J. A. del Alamo and R. M. Swanson, "Modelling of minority-carrier transport in heavily doped silicon emitters," *Solid State Electron.*, vol. 30, no. 11, pp. 1127–1136, Nov. 1987.
[48] A. Suzuki, "High-efficiency silicon space solar cells," *Solar Energ. Mater. Solar Cells*, vol. 50, no. 1–4, pp. 289–303, Jan. 1998.
[49] J. R. Srour, C. J. Marshall, and P. W. Marshall, "Review of displacement damage effects in silicon devices," *IEEE Trans. Nucl. Sci.*, vol. 50, no. 3, pp. 653–670, Jun. 2003.

Ruqiang Bao received the B.S. and M.S. degrees in materials science and engineering from the University of Science and Technology Beijing, Beijing, China, in 2001 and 2004, respectively, and the Ph.D. degree in materials engineering from Rensselaer Polytechnic Institute, Troy, NY, in 2010.

In 2011, he worked on advanced interconnect for back-end-of-line technology strategy as a Postdoctoral Researcher in IBM Research. Currently, he is with the IBM Semiconductor Research and Development Center, Hopewell Junction, NY, working on front-end-of-line, particularly high-k metal gate, for 22-nm-node technology and beyond complementary–metal–oxide semiconductor.

Peter J. Brand received the A.A.S. degree in electrical technology from Hudson Valley Community College, Troy, NY, in 1980 and the B.S. degree in electrical engineering from Rensselaer Polytechnic Institute, Troy, in 1995.

He is currently a Technical Manager at the Rensselaer Polytechnic Institute Linear Accelerator Facility, where he has been for the past 26 years. He provides engineering support for faculty, staff, and researchers and leads the technical team responsible for operation and maintenance of the accelerator. Prior to Rensselaer Polytechnic Institute, he worked as an Electronics Technician and Field Service Representative.

Douglas B. Chrisey received the B.S. degree in physics from Binghamton University-State University of New York, Binghamton, in 1983 and the Ph.D. degree in engineering physics from the University of Virginia, Charlottesville, in 1987.

He spent the next 17 years at the Naval Research Laboratory, Washington, DC. Currently, he is a Professor of materials science and biomedical engineering at Rensselaer Polytechnic Institute, Troy, NY. His research interests include the laser fabrication of thin films of advanced electronics, sensors, biomaterials, and materials for energy storage. These materials were used in device configurations for testing and typically have an improved figure of merit.